Nature Environment and Pollution Technology
An International Quarterly Scientific Journal

p-ISSN: 0972-6268 e-ISSN: 2395-3454	Vol. 16	No. 2	pp. 455-461	2017

Original Research Paper | Open Access

Uncertainty Analysis of Assessing Climate Change Over the North China Plain in the 2050s Using the WRF Model

Ruiping Guo* and Chunlin Yang†**
*Nuclear and Radiation Safety Center, Ministry of Environmental Protection, Beijing, 100082, China
**Henan Institute of Science and Technology, Xinxiang, 453003, China
†Corresponding author: Chunlin Yang

Nat. Env. & Poll. Tech.
Website: www.neptjournal.com

Received: 17-04-2016
Accepted: 24-05-2016

Key Words:
WRF-ARW model
Climate change scenario
Correction methods
The North China plain

ABSTRACT

This study uses a WRF model to simulate the climate for 2000-2008 and the future climate change for 2051-2059 over the North China Plain under A2, A1B, and B1 emission scenarios. To validate the accuracy of a WRF simulation, the global land data assimilation system (GLDAS) data are introduced in this paper. Considering the effectiveness of GLDAS data first is necessary because these data are the products generated by employing satellite and ground-based observational data. The observations of 49 weather stations (MET) over the North China Plain are selected. The spatial-temporal characteristics of temperature and precipitation of GLDAS are highly consistent with those of the MET. A comparison of temperature and precipitation between that of WRF and GLDAS shows that the temperature generated by WRF is overestimated, but the precipitation rate it obtains is consistent with that of GLDAS (R = 0.94). The temperature obtained by WRF that is corrected by a bias correction technique, which is based on the cumulative distribution function, has a high correlation with that of GLDAS. The results of this study can be used to learn the influence of climate change on agriculture and water resources by deriving a crop model and a hydrological model on a regional scale. Results show that the mean temperature will increase by 0.21°C, 1.20°C and 1.55°C; the daily maximum temperature by 0.74°C, 1.76°C and 2.20°C; and the daily minimum temperature by -0.41°C, 0.52°C and 0.79°C under B1, A1B and A2, respectively. On the other hand, to a certain extent, precipitation will decrease by 6.1%, 13.7% and 7.8% under B1, A1B and A2 in the future.

INTRODUCTION

The effects of anthropogenic global warming on regional agriculture and water resources have become an important issue in the past few years (Gregory et al. 2005, Fuhrer et al. 2006). The reliability of results on the relationship between agriculture and climate change depends crucially on high-quality projections of a climate model (Schmidhuber et al. 2007). Therefore, developing climate data with fine resolution is necessary. Recently, a number of works have investigated the application of regional climate models combined with general circulation model (GCM) to research the possible effects of climate change on a regional scale.

In general, global climate models (GCMs), which utilize both global atmospheric and oceanic circulation models, run at coarse resolution and are widely applied on a global scale to predict global climate change (Knight et al. 2004, Naylor et al. 2007, Randall et al. 2007). The Fourth Assessment Report of the Intergovernmental Panel on Climate Change (IPCC) reveals that temperature may increase by approximately 1.4°C-6.4°C, 1.1 °C-2.9°C, 2.0°C-5.4°C and 1.4°C-3.8°C under A1, B1, A2 and B2 at the end of this century under future emission scenarios based on the outputs from GCMs. The warming trend in some regions may be more serious than that at the global level. Accurate prediction at fine spatial resolution is crucial to create an effective knowledge database for addressing regional and local problems and for studying extreme weather and unusual weather patterns on the regional scale (Kueppers et al. 2005, Pierce et al. 2009). To understand and investigate regional climate change, accurate simulations of future climate characteristics using different regional climate models, such as CSIRO CCAM (Nguyen & McGregor 2009), RegCM (Torma et al. 2009), RCM (Kay et al. 2006), WRF model (Zhang et al. 2009), are important.

Intensive studies on the bias correction methodology of climate model results have been conducted to realistically represent future climate changes (Christensen et al. 2008, Piani et al. 2009). Simulations of general and regional climate models cannot be directly used in ecological models without prior bias correction because of the uncertainty and inaccuracy of such climate models (Sharma et al. 2007).

The aim of the present study is to examine the climate change over the North China Plain by focusing mainly on the changes in temperature and precipitation. We use the

outputs of the WRF model for 2000-2008 and in future A2, A1B and B1 climate change scenarios for 2051-2059. The performance of the WRF model is evaluated using GLDAS data, and bias correction is performed on the WRF results based on the statistical distribution. The difference between the corrected and original temperatures is analysed.

METHODOLOGY

Study area: The North China Plain is the second largest plain and is situated on the lower reaches of the Yellow River (31°24'N, 110°18'E-42°42'N, 122°42'E) (Fig. 1). Spreading over an area of approximately 300,000 km^2, this region covers Hebei, Shandong, Henan, Anhui, Jiangsu, Beijing and Tianjin. The region has a warm and semi-humid continental monsoon climate, with an annual mean temperature of 8°C-15°C and an annual precipitation of 600-800 mm. In summer, which consists of hot and wet weather, the maximum temperature during the hottest month (July) is 28°C. In winter, when the weather is cold and dry, the minimum temperature in the area is -6°C-0°C during the coldest month (January).

WRF model: The advanced research WRF (ARW) modeling system used in this study has desirable characteristics; it is designed to be highly modular and can maintain a single source code that can be configured for both research and operations (http://wrf-model.org/index.php). Furthermore, the ARW modeling system is suitable for application in idealized simulations, parameterization research, data assimilation research, forecast research and real-time NWP, and coupled-model applications (Stensrud et al. 2009). In recent studies, the predictive capability of WRF with improved accuracy has been demonstrated by several scientists (Davis et al. 2008, Nicole & Gerhard 2010).

In the present study, the WRF model domain was set up over the North China Plain with the time step of 1800 s and a horizontal resolution of 30 km × 30 km. The initial data for 2000-2008 were from the NCEP/NCAR Global Reanalysis Project (ds090.0) (http:// dss.ucar.edu /datasets /ds090.0 /data /pgbf00-grb2d), with a 2.5° resolution and a time step of 6 h. Given the necessity of SST data when running long simulations and the benefit of updating SST during a model run, the global SST data with a 0.5° resolution were selected (ftp: // polar.ncep.noaa.gov /pub /history /sst (historic 0.5 degree data - only GRIB1)). The drive data in future scenarios under A2, A1B, and B1 for 2051-2059 were generated based on the CCSM simulation results (http:// www.ccsm.ucar.edu/) with a 2.5° resolution and a time step of 6 h (Mo et al. 2013).

Global land data assimilation system (GLDAS): GLDAS data are generated by employing satellite and ground-based observational data products, advanced land surface modeling, and data assimilation techniques (Rodell et al. 2004). GLDAS can supply the optimal fields of land surface states and fluxes and can be downloaded from the website (http://ldas.gsfc.nasa.gov). In this study, monthly Noah data from 2001 to 2008 over North China Plain with a spatial resolution of 0.25° × 0.25° were used to validate the performance of the WRF simulations.

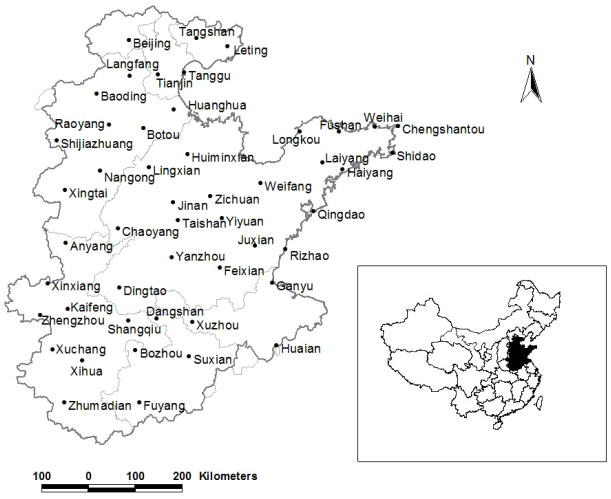

Fig. 1: The distribution of 49 weather stations and the location of North China Plain.

First, we considered whether GLDAS data could accurately describe the weather condition in the North China Plain. The weather data of 49 meteorological stations from 2001 to 2008 were selected to validate the GLDAS data (Fig. 1). Daily observed meteorological data (MET) of the selected 49 meteorological stations were supplied by the China Meteorological Administration.

Bias correction: Bias correction based on the statistic technique was applied in this study (Feddersen & Andersen 2005). In general, the distribution of temperature with time follows the normal distribution. At first, the correction relationship that depends on the quantile is generated by matching the cumulative density function (CDF) of simulations with that of the observation. The correction function is then used to unbias the temperature from the present climate condition and the future climate scenario quantile by quantile.

On the basis of the method detailed above, we separately corrected the temperature simulated by the WRF in the present (T_{HIS}) and future scenarios under A2, A1B, and B1 (T_{A2}, T_{A1B}, T_{B1}). The temperature data of different seasons must be pre-processed with the normalization method (mean = 0, standard error = 1) before the probability distri-

bution could be calculated as T_{GNORM} (GLDAS normalized temperature), $T_{HISNORM}$, T_{A2NORM}, $T_{A1BNORM}$, and T_{B1NORM}. The nine-year average daily temperature was used to obtain the functions of the CDF, while that of WRF in different years could be derived from this CDF. In this paper, the probability of the WRF temperature on some days was assumed to be similar to that of the GLDAS temperature. Thus, the temperature on some days could be corrected by using the GLDAS temperature with the condition that the same probability and formulas are used as follows:

$$T_{HISCOR} = T_{GNORM} \times \delta_{HIS} + \overline{T_G}$$

$$T_{A2COR} = T_{GNORM} \times \delta_{A2} + \overline{T_G} + \overline{T_{A2} - T_G}$$

Here, T_{HISCOR} and T_{A2COR} are the corrected temperature for HIS and A2. δ_{HIS} and δ_{A2} are the standard deviations of HIS and A2. T_{GNORM} is the annual mean normalized temperature.

Temperature correction was applied independently for four seasons [March-May (MAM), June-August (JJA), September-November (SON), and December-February (DJF)], because the temperature bias between WRF and GLDAS depends on the change of seasons. To show the difference between the CDFs of GLDAS and of WRF, the domain center grid was taken as an example. The CDFs of temperature in four seasons of GLDAS and WRF are shown in Fig. 2. The figure shows significant differences in different seasons. The largest difference of CDF between GLDAS and WRF occurs in summer (JJA). However, the differences in autumn and in winter were smaller. The CDFs of temperature under the B1, A1B, and A2 emission scenarios had similar variation trends with time to those under the current climate (2000-2008). However, obvious warming trends in summer and winter were observed.

RESULTS AND DISCUSSION

Validation of GLDAS with MET: To evaluate the performance of GLDAS data, the temporal and spatial patterns of MET data obtained from 49 weather stations were applied. Statistical analysis showed that the annual mean temperature and annual precipitation (287.00±1.50 K and 695.1±181.0 mm respectively) of the 49 MET stations were consistent with those of GLDAS (287.23±1.42 K and 684.1±203.9 mm respectively). To provide the details, the region was divided into three parts from north to south with

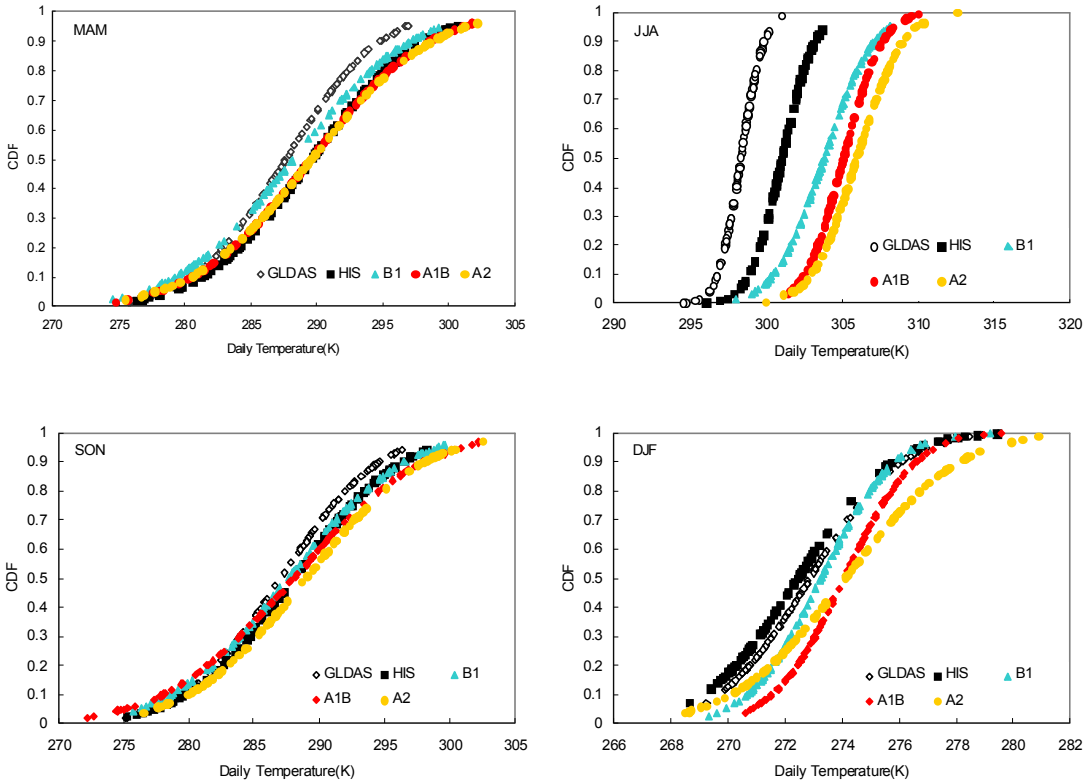

Fig. 2: The CDFs of daily temperature of GLDAS and WRF in the domain center (16, 14) in different seasons under current, B1, A1B and A2.

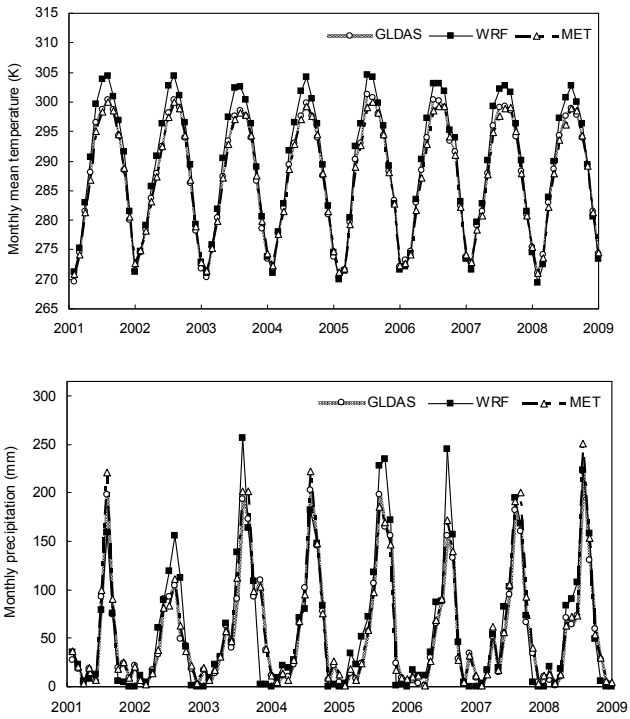

Fig. 3: The temporal characters of monthly mean temperature and monthly precipitation of GLDAS, MET and WRF.

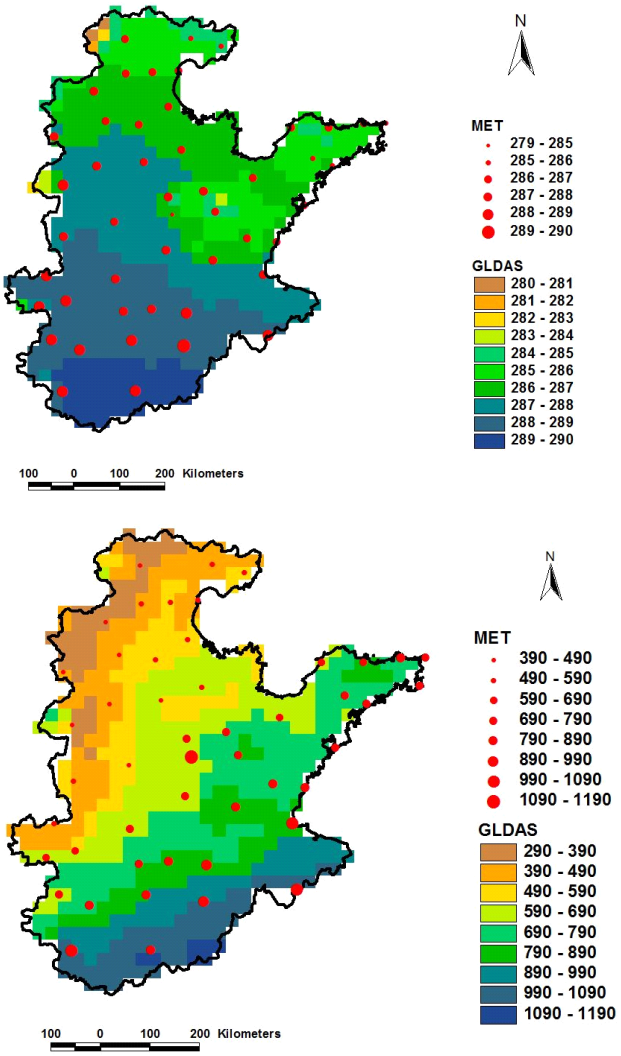

Fig. 4: Spatial distributions of annual mean temperature (K) (top) and annual precipitation (mm) (below) for GLDAS and MET.

the same latitude intervals. In the northern part, the temperature of GLDAS (285.86±1.07 K) was near to that of MET (286.38±0.68 K), but the precipitation of GLDAS (494.0±128.7 mm) was about 10.8% lower than that of MET (553.5±102.8 mm). In the middle part, the temperature of GLDAS (286.93±1.07 K) was also close to that of MET (286.57±1.77 K), and the precipitation of GLDAS (639.5±124.3 mm) presented the same trend as that in the North, but the recorded precipitation was approximately 9.5% lower than that of MET (707.0±178.5 mm). In the southern part, the temperatures obtained by GLDAS (288.66±0.56 K) and MET (288.43±0.44 K) were similar, but the precipitation recorded by GLDAS (885.3±148.6 mm) was obviously higher than that of MET (850.2±121.7 mm) by approximately 4.1%. The findings showed no obvious difference in temperature and precipitation between GLDAS and MET for the entire region, but a variation in precipitation in different parts was exhibited.

The changes in monthly mean temperature and precipitation with time were analysed to further reflect the characteristics of climate seasonal change (Fig. 3). The GLDAS data had higher correlation with the MET data (the temperature and precipitation were 0.998 and 0.992 respectively). Furthermore, the spatial distributions of temperature and precipitation of GLDAS were similar to those of MET. A considerable increase in temperature and precipitation of both GLDAS and MET occurred from northwest to southeast (Fig. 4). Many similarities exist between the GLDAS data and MET data, not only in temporal variation but also in spatial distribution. Therefore, GLDAS data over the North China Plain have high creditability and can be used to evaluate the WRF simulations as the observation data.

Comparison of GLDAS and WRF: A synthetic view of the performance of WRF simulation compared with GLDAS is shown in Fig. 5. The temperature bias is the difference between WRF and GLDAS, and the precipitation bias is the change percent of WRF relative to that of GLDAS. The temporal variation of temperature bias is evident and has a similar trend with the seasonal change of temperature. The most

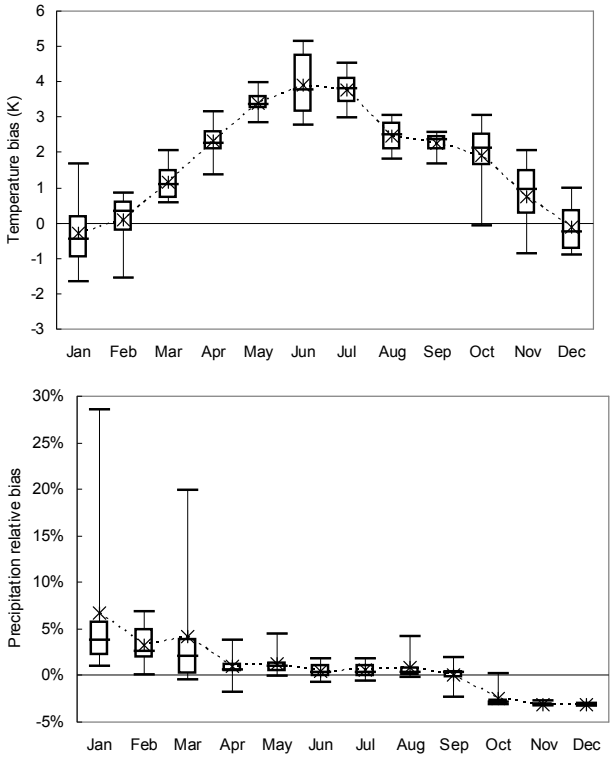

Fig. 5: Biases of temperature and precipitation between GLDAS and WRF during 2001-2008 (star stands for mean condition).

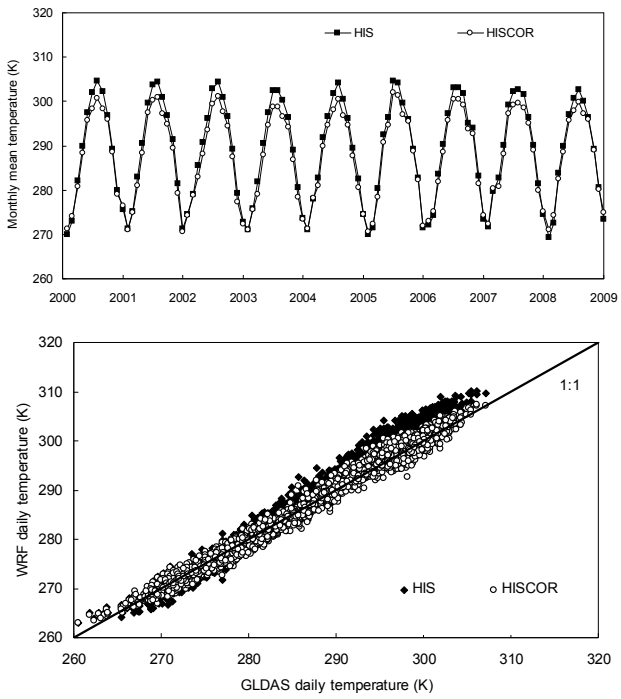

Fig. 6: The corrected WRF temperature and the relationship between HIS, HISCOR and GLDAS in history.

important bias is obtained in summer (approximately 3.4°C), with a general overestimation of WRF temperature compared with the GLDAS observation. In winter, the temperature bias is smallest and changes around 0°C. For precipitation, the temporal change of precipitation bias is opposite to that of temperature and a larger decrease in precipitation occurs in winter than in summer. The underestimation of WRF precipitation in winter may be caused by the extremely small simulations of the WRF model. High variations of the precipitation bias between WRF and GLDAS in different years over the period 2001-2008 are observed.

The difference analysis between the corrected and original temperature: Large biases of WRF temperature were found by comparing the temperature and precipitation between GLDAS and WRF. Thus, correcting the simulation results of WRF was necessary. Fig. 6 illustrates the temperature variation of history condition (HIS) and corrected value in history (HISCOR) with time (Mo et al. 2013). As shown in the figure, the temporal change of corrected temperature has a commonality with that of GLDAS, being obviously lower than before without bias correction in summer. For spatial distribution, the correlation between corrected daily temperature (HISCOR) and GLDAS is also very high, which is close to 1:1 line. Before correction, the WRF temperature showed the overestimation when temperature was greater than 285 K.

With the domain center as an example, Fig. 7 presents the variation characters of temperature before and after correction in different seasons with time under current scenario and A2. The corrected temperature in the current scenario not only keeps the similar average level with GLDAS data, but also maintains the daily variability of WRF simulation. In summer in particular, the corrected temperature is less than that without bias correction. Under the A2 climate scenario, the corrected temperature in summer is also less than before, but that in winter is slightly higher than before.

CONCLUSIONS

The WRF model was used to explore the temporal and spatial pattern of current climate and possible future climate change over the North China Plain. The present climate over the period 2000-2008 and the A2, A1B, and B1 future climate scenarios over the period 2051-2059 were simulated by the WRF model initialized by the NCEP data and the CCSM global climate model projected data.

The result of the comparison between WRF and GLDAS demonstrates that the temperature obtained by WRF was overestimated relative to the observation, particularly in summer, but the precipitation obtained by WRF was similar

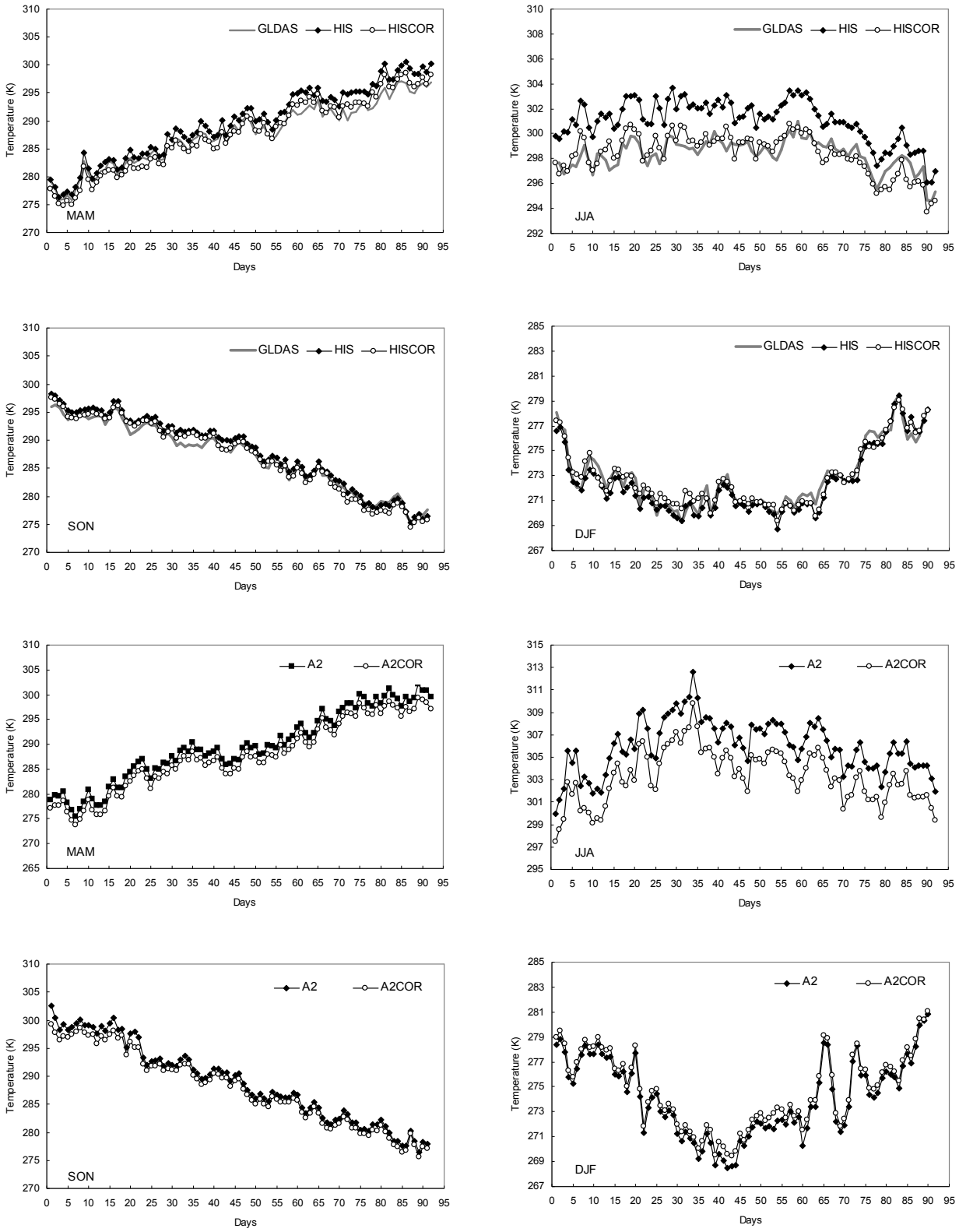

Fig. 7: The temporal variations of daily temperature of GLDAS, HISCOR and A2COR in the domain center (16, 14) for different seasons.

to that of GLDAS. Bias correction method was applied to solve the bias problem, which was based on the cumulative PDF of WRF simulation, that is the same as that of GLDAS observation.

For the North China Plain, an overall increase in mean temperature of 0.21°C, 1.20°C, and 1.55°C; daily maximum temperature of 0.74°C, 1.76°C, and 2.20°C; and daily minimum temperature of -0.41°C, 0.52°C, and 0.79°C under B1, A1B, and A2 future climate scenarios relative to the present were predicted. The annual mean precipitation in the future presented a significantly decreasing trend, and the precipitation was predicted to decrease by 6.1%, 13.7%, and 7.8 % under B1, A1B, and A2.

This work illustrated the possible climate change over the North China Plain. As revealed by this study, future climate change in the area will be significant, and studying such change is necessary to mitigate its effects on the ecological functions of the region. The simulations performed in this study can be used to derive a crop model, a hydrological model, and an ecological model to study the effects of climate change on agriculture.

ACKNOWLEDGEMENTS

This research is supported by CAP1400 Safety Review Key Technology Research (2013ZX06002001).

REFERENCES

Christensen, J.H., Boberg, F., Christensen, O.B. and Lucas-Picher, P. 2008. On the need for bias correction of regional climate change projections of temperature and precipitation. Geophys. Res. Lett., 35(20).

Davis, C., Wang, W., Chen, S.S., Chen, Y., Corbosiero, K., DeMaria, M., Dudhia, J., Holland, G., Klemp, J., Michalakes, J., Reeves, H., Rotunno, R., Snyder, C. and Xiao, Q. 2008. Prediction of landfalling hurricanes with the advanced hurricane WRF model. Mon. Wea. Rev., 136: 1990-2005.

Feddersen, H. and Andersen, U. 2005. A method for statistical downscaling of seasonal ensemble predictions. Tellus A, 57(3): 398-408.

Fuhrer, J., Beniston, M., Fischlin, A., Frei, C., Goyette, S., Jasper, K. and Pfister, C. 2006. Climate risks and their impact on agriculture and forests in Switzerland. Climatic Change, 79: 79-102.

Gregory, P.J., Ingram, J.S.I. and Brklacich, M. 2005. Climate change and food security. Philos. T. Roy. Soc. B., 360: 2139-2148.

Kay, A.L., Jones, R.G. and Reynard, N.S. 2006. RCM rainfall for UK flood frequency estimation. II. Climate change results. Journal of Hydrology, 318(1-4): 163-172.

Knight, M., Thomas, D.S.G., Wiggs, G.F.S. 2004. Challenges of calculating dunefield mobility over the 21st century. Geomorphology, 59: 197-213.

Kueppers, L.M., Snyder, M.A., Sloan, L.C., Zavaleta, E.S. and Fulfrost, B. 2005. Modeled regional climate change and California endemic oak ranges. PNAS, 102(45): 16281-16286.

Mo, X.G., Guo, R.P., Liu, S.X., Lin, Z.H. and Hu, S. 2013. Impacts of climate change on crop evapotranspiration with ensemble GCM projections in the North China Plain. Climatic Change, 120: 299-312.

Naylor, R.L., Battisti, D.S., Vimont, D.J., Falcon, W.P. and Burke, M.B. 2007. Assessing risks of climate variability and climate change for Indonesian rice agriculture. PNAS, 104(19): 7752-7757.

Nguyen, K.C. and McGregor, J.L. 2009. Modelling the Asian summer monsoon using CCAM. Clim. Dyn., 32: 219-236.

Nicole Mölders, N. and Krammb, G. 2010. A case study on wintertime inversions in interior Alaska with WRF. Atmospheric Research, 95(2-3): 324-332.

Piani, C., Coppola, E., Mariotti, L., Haerter, J. and Hagemann, S. 2009. A statistical bias correction for climate model data: parameter sensitivity analysis. Geophysical Research Abstracts, 11: EGU2009-8034.

Pierce, D.W., Barnett, T.P., Santer, B.D. and Gleckler, P.J. 2009. Selecting global climate models for regional climate change studies. PNAS, 106(21): 8441-8446.

Randall, D.A., Wood, R.A., Bony, S., Colman, R., Fichefet, T., Fyfe, J., Kattsov, V., Pitman, A., Shukla, J., Srinivasan, J., Stouffer, R.J., Sumi, A. and Taylor, K.E. 2007. Climate models and their evaluation. In: Climate change 2007: The physical science basis. Contribution of Working Group I to the Fourth Assessment Report of the IPCC (FAR). Cambridge University Press, pp. 589-662.

Rodell, M., Houser, P.R., Jambor, U., Gottschalck, J., Mitchell, K., Meng, C.J., Arsenault, K., Cosgrove, B., Radakovich, J., Bosilovich, M., Entin, J.K., Walker, J.P., Lohmann, D. and Toll, D. 2004. The Global land data assimilation system. Bull. Amer. Meteor. Soc., 85(3): 381-394.

Schmidhuber, J. and Tubiello, F.N. 2007. Global food security under climate change. Proc. Natl. Acad. Sci. USA, 104(50): 19703-19708.

Sharma, D., Gupta, A.D. and Babel, M.S. 2007. Spatial disaggregation of bias-corrected GCM precipitation for improved hydrologic simulation: Ping river basin, Thailand. Hydrol. and Earth Sys. Sci., 11(4): 1373-1390.

Stensrud, D.J., Yussouf, N., Dowell, D.C. and Coniglio, M.C. 2009. Assimilating surface data into a mesoscale model ensemble: Cold pool analyses from spring 2007. Atmospheric Research, 93: 207-220.

Torma, C.S., Bartholy, J., Pongracz, R., Barcza, Z., Coppola, E. and Giorgi, F. 2009. Estimation of regional climate change in the Carpathian basin using RegCM simulations for A1B scenario. Geophysical Research Abstract, 11: EGU2009-12319-1.

Zhang, Y.X., Dulière, V., Mote, P. and Salathé, Jr E.P. 2009. Evaluation of WRF and HadRM mesoscale climate simulations over the United States Pacific Northwest. Journal of Climate, 22(20): 5511-5526.